Periodica Polytechnica Mechanical Engineering, 70(1), pp. 76–81, 2026

NURBS-based Reverse Engineering of the Mandible, Creation of a Layered 3D Model Based on Real CT Scans

Klaudia Papp[1*], István Attila Piros[2], Zsolt Tégla[3]

[1] Department of Machine and Product Design, Faculty of Mechanical Engineering, Budapest University of Technology and Economics, Műegyetem rkp. 3., H-1111 Budapest, Hungary
[2] Department of Innovative Vehicles and Materials, Neumann János University, Izsáki út 10., H-6000 Kecskemét, Hungary
[3] Department of Economics, Keleti Károly Faculty of Business and Management, Óbuda University, Tavaszmező utca 17., H-1084 Budapest, Hungary
[*] Corresponding author, e-mail: papp.klaudia@nje.hu

Received: 15 December 2025, Accepted: 21 January 2026, Published online: 19 February 2026

Abstract

This paper presents the high-resolution reconstruction of a human mandible and lower dentition based on real CT data. The primary goal was to create a continuous spline-based computer model that provides a robust foundation for analyzing the tooth–bone interface. Special emphasis was placed on the realistic integration of teeth into the mandible, enabling the model to be divided into distinct biological layers. The resulting geometry is fully prepared for numerical simulations, where individual solid parts can be assigned specific material properties, allowing more accurate finite element analysis of the mechanical behavior of different regions.

Keywords

mandible, FEA, reverse engineering, medical imaging

1 Introduction

Accurate computer-based reconstruction of anatomical structures is a cornerstone of modern biomechanical research. This project focuses on developing a high-resolution 3D model of the human mandible and dentition based on real CT data. Unlike simplified representations, the model provides a layered and parameterized geometry, enabling detailed finite element analysis (FEA). By assigning distinct material properties to cortical bone, spongiosa, enamel, dentin, and cementum, the reconstruction supports anatomically realistic simulations of tooth–mandible interactions, particularly in the context of dental prosthesis design.

The workflow involves CT image segmentation, NURBS-based surface reconstruction, and solid model generation, resulting in a smooth, topologically consistent structure optimized for meshing and mechanical analysis. Previous studies have often relied on tessellated geometries, which limit mesh flexibility and reduce the accuracy of stress distribution analysis. Moreover, many existing mandibular models neglect the detailed representation of the tooth–bone interface, even though this region plays a critical role in load transfer and prosthetic evaluation. Addressing this gap, special emphasis is placed on modeling the tooth–bone connection, which allows the investigation of both static load distribution and dynamic masticatory processes. The outcome is a modular, simulation-oriented model that provides a robust foundation for biomechanical studies and contributes to more precise approaches in the planning and evaluation of dental prostheses.

2 Preparation and processing of CT data

High-precision biomechanical modeling requires reliable medical imaging data. For this study, cone-beam CT scans of the mandible were acquired at the Faculty of Dentistry, University of Szeged, using a Gendex GXDP-800 device. The images were recorded with Gendex VixWin Platinum software and exported in standard DICOM format, which contains both image slices and related metadata [1]. For the 3D reconstruction, 9 sagittal, 7 axial, and 5 coronal slices of a single participant were utilized to capture the detailed geometry of the mandibular region and dentition.

2.1 Loading and pre-filtering of DICOM data

The imported DICOM dataset was visually and technically screened to isolate the mandibular region and denti-

Cite this article as: Papp, K., Piros, I. A., Tégla, Z. "NURBS-based Reverse Engineering of the Mandible, Creation of a Layered 3D Model Based on Real CT Scans", Periodica Polytechnica Mechanical Engineering, 70(1), pp. 76–81, 2026. https://doi.org/10.3311/PPme.43104

tion [2, 3]. Irrelevant slices and artifacts were excluded to ensure that subsequent reconstruction steps were based solely on meaningful anatomical information (Fig. 1).

2.2 Image enhancement: noise reduction and contrast adjustment

Raw CT images are frequently affected by noise and insufficient contrast, especially when distinguishing between tissues with similar density (e.g., cortical vs. spongy bone, dentin *vs*. cementum). To improve segmentation reliability, a 3 × 3 Gaussian smoothing filter ($\sigma = 1.0$) was applied to reduce high-frequency noise [4], followed by a median filter with kernel size 3 × 3 to eliminate isolated artifacts while preserving edges [4]. For contrast enhancement, global histogram equalization was applied consistently to all image slices, ensuring uniform sharpening of structural boundaries across the dataset. These preprocessing steps significantly improved the separation between tissue layers, providing a more accurate foundation for NURBS-based surface reconstruction and ensuring that the final 3D model closely reflects anatomical reality [5].

3 Segmentation and 3D reconstruction

An essential step in creating a reliable biomechanical model is segmentation, where the mandible and dentition are separated from surrounding tissues in CT images. This process guarantees the level of accuracy and anatomical precision necessary for reliable 3D modeling and finite element analysis (FEA) [6].

3.1 Separation of bone and soft tissues (3D slicer)

The Segmentation was performed using the medical imaging software 3D Slicer, which supports DICOM-based 3D data processing. Bone tissues (cortical and spongy bone) were isolated from soft tissues through intensity-based thresholding. Manual refinements were applied in regions where automatic methods could not capture fine anatomical details of the teeth and mandible [7, 8].

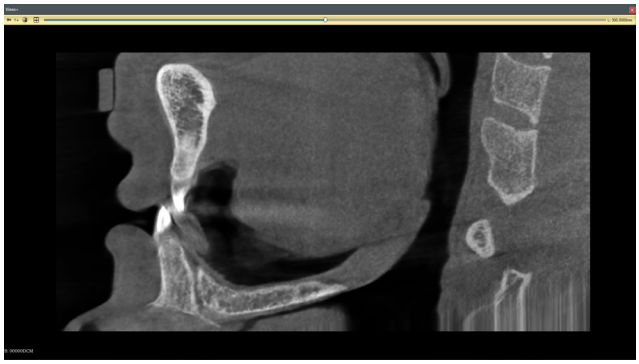

Fig. 1 Sagittal section of the mandible on CT scan

As a result, distinct regions were generated for the bony structures, teeth, and – where possible – surrounding soft tissues [9]. Accuracy was verified across multiple imaging planes (axial, sagittal, coronal), and boundaries were refined to ensure anatomical consistency (Figs. 2 and 3). Quantitatively, the reconstructed contours showed a maximum deviation of less than 0.2 mm from the reference CT slices, with an average Root Mean Square Error (RMSE) of 0.08 mm, confirming the geometric fidelity of the model.

3.2 Generation of tessellated 3D geometry

Following segmentation, surface representations of each region were produced as triangular meshes, exported in STL format for CAD and FEA applications. The voxel-based CT data served as the basis for isosurface extraction, yielding geometries that reflect the anatomical surfaces. The original mesh consisted of 2,557,328 facets with an average edge length of 0.8 mm, which was then simplified using the decimate function, retaining 4.3% of the elements. The resulting base geometry contained 110,182 facets with an average edge length of 2.5 mm, providing a balance between anatomical fidelity and computational efficiency (Fig. 4).

To improve mesh quality, curvature-based remeshing refinement was applied, which adaptively increased mesh resolution in regions of high geometric complexity while preserving smoother areas with lower element density.

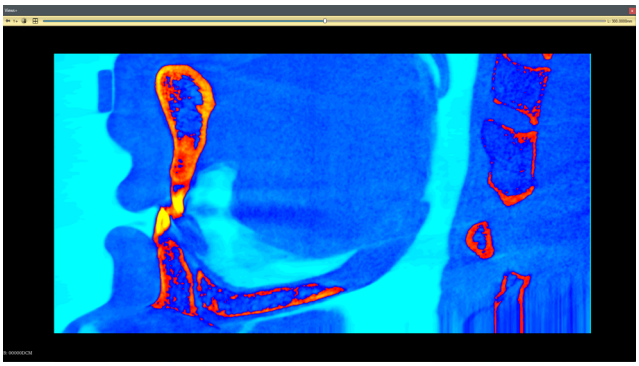

Fig. 2 Segmented sagittal section of the mandible [1]

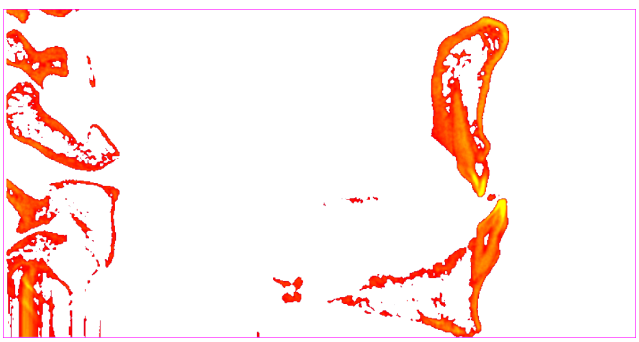

Fig. 3 Segmented sagittal section of the mandible without background

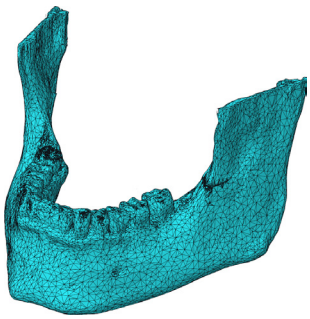

Fig. 4 CT scan model of the mandible [1]

Additional error correction steps included closing surface holes with a maximum diameter of 0.5 mm, removing isolated points smaller than 3 connected triangles, and applying surface smoothing with a tolerance of 0.2 mm to reduce irregularities without distorting anatomical accuracy [10]. The resulting tessellated model thus provided a robust and topologically consistent foundation for subsequent NURBS-based reconstruction and the creation of a parameterized CAD model.

In contrast, CAD/CAM requires more upfront planning but can be applied to any mandibular defect and location, including the condyle. Additionally, CAD/CAM is versatile, enabling its use for other microvascular bone transplants, such as scapula or iliac crest grafts [10].

4 Spline-based surface reconstruction

While tessellated CT-based geometries are suitable for visualization, they are too coarse and non-parametric for biomechanical simulations. To achieve a smooth, editable, and simulation-ready model, the mesh was refined and reconstructed using Non-Uniform Rational B-Splines (NURBS) within PTC Creo 11.

4.1 NURBS surface creation in CAD environment

The STL mesh exported from 3D slicer served as a reference for defining spline curves in sagittal (6 curves), axial (7 curves), and cortical (10 curves) planes (Fig. 5). These splines, constructed with an average control point spacing of 7 mm and degree-5 polynomial functions, were fitted along the inner and outer contours of the mandible and teeth to ensure continuity and smoothness. Based on these curves, NURBS surfaces were generated using a structured patch layout: In the case of the mandible, 30 patches were created. The parametrization followed chord-length assignment as provided by Creo, and G1 continuity (tangential smoothness) was maintained across adjacent patches [11]. Manual fitting was applied without automated tolerance control, yielding an average deviation of ±0.2 mm from the STL reference surface. Additional smoothing was limited to tangent alignment at curve start and end vectors, ensuring seamless transitions without altering the geometric fidelity.

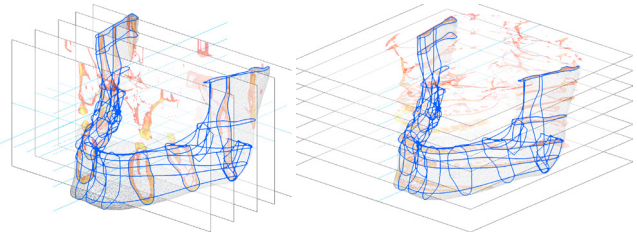

(a) (b)

Fig. 5 Alignment of cortical (a) and axial (b) CT sections with the mandible described by curves

Validation was carried out by projecting the reconstructed model back onto the tessellated mesh. Both visual inspection and numerical analysis confirmed the accuracy of the NURBS-based geometry: the maximum deviation from the reference tessellated surface was 0.18 mm, with an average Root Mean Square Error (RMSE) of 0.08 mm. These results demonstrate that the reconstructed model closely matches the anatomical form while providing superior smoothness and editability for subsequent FEA (Figs. 6 and 7).

4.2 Model decomposition by biological layers

The mechanical behavior of the mandible depends not only on geometry but also on internal structural differentiation. Based on CT intensity distribution, two main bone regions were modeled separately:

- Cortical bone: dense outer layer.
- Spongiosa: porous inner structure [12].

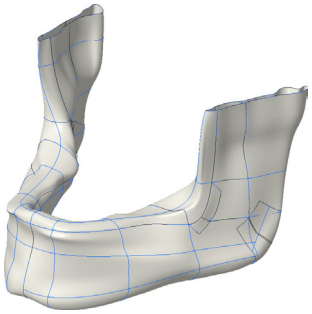

Fig. 6 The final mandible model [1]

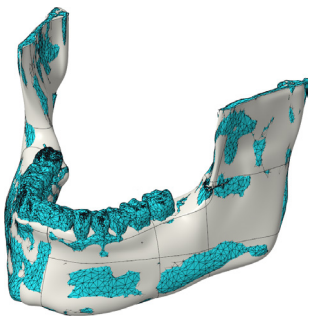

Fig. 7 The merged CT scan and the final mandible model [1]

To distinguish these regions, a thresholding range of > +450 HU for cortical bone and between +150 and +450 HU for spongiosa was applied. The CT images had a voxel size of 0.3 × 0.3 × 0.3 mm^3 and a slice thickness of 0.3 mm, ensuring sufficient resolution to capture boundary transitions. Using reference curves, distinct surface models were generated for each region in PTC Creo, with their boundaries defined by anatomical landmarks and density variations. During solid generation, a maximum geometric deviation tolerance of ±0.2 mm was maintained to preserve anatomical fidelity.

In preparation for finite element analysis, literature-based mechanical properties were assigned to the two bone regions (Fig. 8). These values are summarized in Table 1.

This layer-based approach also establishes a framework for integrating dental structures, leading to a comprehensive, parameterized, and simulation-oriented model of the mandible and dentition.

5 Development of an integrated tooth–mandible model

Accurate representation of the tooth–mandible connection is essential for realistic biomechanical simulations. Integration of teeth into the mandibular model required anatomically correct positioning, while also ensuring morphological and mechanical consistency.

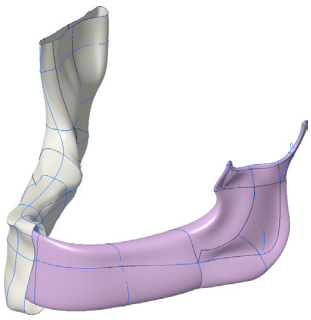

Fig. 8 Location of the spongiosa layer in the cortical layer

Table 1 The material properties of the layers [1]

Material properties/layers	Cortical bones	Spongiosa
Density	1.8 g/cm^3	1.87 g/cm^3
Young-modulus	14,500 MPa	1,370 MPa
Poisson's ratio	0.323	0.3
Shear-modulus	5,480 MPa	527 MPa
Bulk-modulus	13,650 MPa	1,140 MPa
Isotropic secant coefficient of thermal expansion	27.5·10^{-6} 1/°C	27.5·10^{-6} 1/°C
Tensile Ultimate Strength	60 MPa	2.22 MPa
Tensile Yield Strength	55 MPa	2.12 MPa
Compressive Yield Strength	117 MPa	2.54 MPa
Compressive Ultimate Strength	130 MPa	2.44 MPa

5.1 Tooth placement in the mandible

After reconstructing the teeth separately, they were positioned and oriented within the mandible using root canals and sockets visible on CT scans as references. The alignment was guided by segmented contours and NURBS-based mandibular surfaces, ensuring a natural dental arch and the absence of gaps or overlaps, which is critical for finite element meshing [13].

5.1.1 Tooth modeling

Each tooth was modeled as an individual solid, aligned with the mandible. Geometries were reconstructed from CT-based contours to reflect the anatomy of incisors, canines, and molars, including detailed crown morphology [13]. The internal structure was layered into enamel, dentin, and cementum, enabling differentiated material properties in later analyses (Fig. 9).

The geometry was built with smooth NURBS surfaces to accurately capture root canal and apex positions, which are key to force transmission [13]. For tooth reconstruction, spline curves were defined in sagittal, axial, and coronal planes – 6, 7, and 10 curves respectively – with an average control point spacing of 7 mm and fifth-degree splines to ensure smooth curvature. The resulting surfaces were assembled from quadrilateral NURBS patches, with approximately 11 patches per single-rooted tooth and 33 patches per double-rooted tooth, maintaining G1 tangency continuity at patch boundaries. A maximum geometric deviation of ±0.2 mm from the reference STL mesh

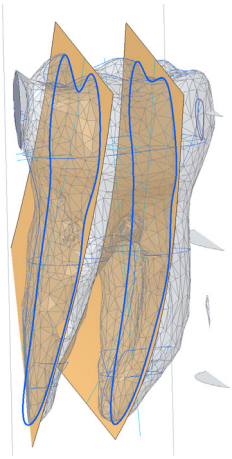

Fig. 9 Sections and curves created from the cortical view

was allowed, and manual tangency adjustments were applied at curve endpoints to refine surface smoothness.

As a result, each tooth became a modular component of the integrated mandibular model, prepared for FEA-based structural analysis with anatomically faithful root canal and apex representation (Fig. 10).

5.2 Geometry validation and error correction

Following integration, the complete model was checked for topological consistency. Validation steps included:

- Surface continuity: ensuring smooth transitions at tooth–mandible interfaces, with a maximum deviation of ±0.2 mm between adjacent surfaces.
- Closed volumes: verifying watertight solids for simulation readiness, with all surface holes successfully closed (≤ 0.5 mm diameter).
- Overlap prevention: confirming that no intersections occurred between teeth and bone, with clearance maintained within the ±0.2 mm tolerance range [13].

Errors were detected and corrected using PTC Creo's Geometry Check and Import Data Doctor tools, which resolved open edges, redundant vertices, and self-intersections. The final continuous and closed model is thus suitable for layer-based material assignment and reliable finite element simulations (Fig. 11).

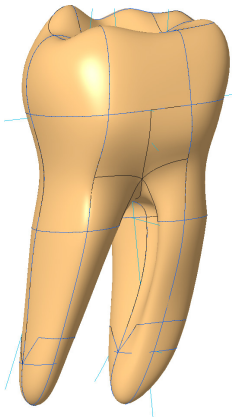

Fig. 10 3D model of the tooth

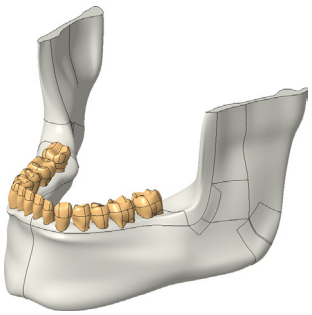

Fig. 11 Teeth remodeled in the mandible

6 Conclusion

The objective of this study was to develop a detailed computational model of the mandible and lower dentition derived from real medical imaging data. The emphasis was placed not only on achieving high anatomical accuracy but also on constructing a layered, material-specific structure that is suitable for biomechanical simulations.

CT scans were processed and segmented in 3D Slicer, followed by triangular mesh tessellation and NURBS-based surface reconstruction in PTC Creo 11. The model was divided into biological layers – cortical and trabecular bone, as well as enamel, dentin, and cementum. Teeth were reconstructed separately and integrated into the mandible with both morphological and biomechanical considerations. Topological errors were corrected to ensure watertight solid behavior.

The final model fully satisfies the requirements of finite element analysis (FEA): it is solid-based, parameterized, layered, and composed of modular units with assignable material properties. This allows for realistic simulations of loading and deformation, including the evaluation of dental prostheses and implants.

The presented reverse engineering workflow not only demonstrates practical modeling methods but also lays the foundation for a complex biomechanical research framework, connecting medical imaging, CAD modeling, and numerical simulations. The developed mandible model can serve as a starting point for further research in dental biomechanics and medical device design.

References

[1] Papp, K., Piros, I. A., Deák, B. "High quality geometric reconstruction of human mandible", MM Science Journal, 2024(Spec. Issue), pp. 7664–7670, 2024. https://doi.org/10.17973/MMSJ.2024_11_2024096

[2] Gradl, R., Zanette, I., Ruiz-Yaniz, M., Dierolf, M., Rack, A., Zaslansky, P., Pfeiffer, F. "Mass Density Measurement of Mineralized Tissue with Grating-Based X-Ray Phase Tomography", PloS ONE, 11(12), e0167797, 2016. https://doi.org/10.1371/journal.pone.0167797

[3] Yuan, T., Liao, W., Dai, N., Cheng, X., Yu, Q. "Single-Tooth Modeling for 3D Dental Model", International Journal of Biomedical Imaging, 2010(1), 535329, 2010. https://doi.org/10.1155/2010/535329

[4] Sunitha, M. R., Asha, D. "Comparison of Gaussian and Median Filters to Remove Noise in Dental Images", Institute of Scholars (InSc), pp. 1430–1436, 2020. [online] Available at: https://papers.ssrn.com/sol3/papers.cfm?abstract_id=3669634 [Accessed: 20 January 2026]

[5] Higuera Garrido, A., Pando Cerra, P., Osorio Zapico, A., Garcia Lopez, M. D. "Obtención de datos geométricos en imagen médica" (Geometric data collection in medical imaging), Dyna, 86(2), pp. 222–231, 2011. (in Spanish)
https://doi.org/10.6036/3868

[6] AlZu'bi, S., Jararweh, Y., Al-Zoubi, H., Elbes, M., Kanan, T., Gupta, B. "Multi-orientation geometric medical volumes segmentation using 3D multiresolution analysis", Multimedia Tools and Applications, 78(17), pp. 24223–24248, 2019.
https://doi.org/10.1007/s11042-018-7003-4

[7] Fang, S., Nowinski, W. L., Jagannathan, L., Srinivasan, R. "Geometric model reconstruction from cross sections for branched structures in medical applications", In: SPIE's 1995 International Symposium on Optical Science, Engineering, and Instrumentation, San Diego, CA, USA, 1995, pp. 329–340. ISBN 0-8194-1932-X
https://doi.org/10.1117/12.216426

[8] Lentge, F., Jehn, P., Neuhaus, M.-T., Bettag, S. A., Gellrich, N. C., Korn, P. "A Novel Method for Secondary Mandible Reconstruction to Re-Achieve a Native Condyle Position Comprising a New Design for Cutting Guides and New Positioning Devices", Journal of Personalized Medicine, 14(2), 181, 2024.
https://doi.org/10.3390/jpm14020181

[9] Wang, C.-S., Lin, M.-C., Wang, C.-C., Chen, C.-F., Hsieh, J.-C. "Feature reconstruction for 3D medical images processing", In: 2013 6th International Conference on Biomedical Engineering and Informatics, Hangzhou, China, 2013, pp. 69–74. ISBN 978-1-4799-2761-6
https://doi.org/10.1109/BMEI.2013.6746909

[10] Denk, L., Sigwart, A.-M., Kolk, A., Walch, B. "Clinical Comparison of CAD/CAM vs. KLS L1® Mandible ReconGuide in Fibula Free Flap Mandible Reconstruction: A Retrospective Clinical Study", Journal of Clinical Medicine, 14(3), 736, 2025.
https://doi.org/10.3390/jcm14030736

[11] Lee, Z.-H., Shuck, J. W., Largo, R. D., Chang, E. I., Hanasono, M. M., Yu, P., Garvey, P. B. "Free fibula mandible reconstruction for osteoradionecrosis is more challenging than for primary cancer", Head & Neck, 46(11), pp. 2834–2842, 2024.
https://doi.org/10.1002/hed.27823

[12] Zhang, Y.-R., Du, W., Zhou, X.-D., Yu, H.-Y. "Review of research on the mechanical properties of the human tooth", International Journal of Oral Science, 6(2), pp. 61–69, 2014.
https://doi.org/10.1038/ijos.2014.21

[13] Tomita, Y., Ichikawa, Y., Hashizume, K., Sakuma, H. "Effect of Gaussian Smoothing Filter Size for CT-Based Attenuation Correction on Quantitative Assessment of Bone SPECT/CT: A Phantom Study", Journal of Digital Imaging, 36(5), pp. 2313–2321, 2023.
https://doi.org/10.1007/s10278-023-00864-3